

LoRa Preamble Detection with Optimized Thresholds

Jae-Mo Kang, *Member, IEEE*

Abstract—LoRa (Long Range) is one of the widely adopted techniques for Internet-of-Things (IoT). Preamble detection is a key initial task for LoRa systems. Meanwhile, the so-called threshold-based preamble detection is a common technique for compatibility with LoRa. However, the existing methods on the threshold-based LoRa preamble detection suffer from low performance because the detection thresholds are heuristically chosen. To tackle this issue, in this letter, we aim to optimize those thresholds by maximizing the preamble detection probability while satisfying a constraint on false alarm rate. For this purpose, coherent and non-coherent procedures for the preamble detection are presented in a universal manner, followed by conducting their performance analysis. Simulation results demonstrate the superiority and effectiveness of the proposed scheme.

Index Terms—Detection, Internet-of-Things (IoT), LoRa, preamble.

I. INTRODUCTION

LoRa (Long Range) based on chirp spread spectrum is a widely adopted technique developed for Internet-of-Things (IoT) [1]. One of the important initial tasks in operating a LoRa system is to detect the presence of preamble, also known as the *preamble detection* [2]–[5], of which result (or success) critically affects subsequent major tasks such as synchronization, channel estimation, and demodulation.

In [2], the theoretical optimal performance of LoRa preamble detection was investigated. To achieve such optimal performance, however, the hardware complexity needs to increase inevitably (such as due to matrix inversion and averaging), eventually leading to incomplete compatibility with LoRa. Moreover, in [2], the impact of fading channel, which is inevitable in a realistic wireless propagation environment, was not taken into account on the preamble detection.

A more compatible strategy with LoRa is the so-called threshold-based preamble detection [3]–[5], which tries to directly discover the presence of the preamble by following the standard reception technique of LoRa, i.e., the process of dechirping, followed by taking discrete Fourier transform (DFT). The key to the threshold-based LoRa preamble detection is comparing the detection results to some thresholds. In [3]–[5], few simple rules of thumbs were established for determining the thresholds; however, the resulting performance is not satisfactory due to their strict suboptimality (i.e., lack of considering the optimization of thresholds). Also, the issue of false alarm was not considered therein.

Motivated by these issues and to improve the performance of the threshold-based preamble detection for LoRa, in this letter, we aim at optimizing the detection thresholds by maximizing the preamble detection probability with a constraint on false alarm rate. To this end, a universal algorithm for both coherent and non-coherent procedures of the threshold-based LoRa preamble detection is first presented. Then, for the first time, analytical expressions of the preamble detection probability and false alarm rate for the threshold-based LoRa preamble detection are derived in closed forms. Simulation results demonstrate that the proposed scheme notably outperforms several comparable baseline schemes considering [3]–[5].

This work was supported in part by Basic Science Research Program through the National Research Foundation of Korea(NRF) funded by the Ministry of Education(2020R111A3073651), and in part by the Korea Institute of Energy Technology Evaluation and Planning(KETEP) and the Ministry of Trade, Industry & Energy(MOTIE) of the Republic of Korea (No. 20224000000150).

J.-M. Kang is with the Department of Artificial Intelligence, Kyungpook National University, Daegu 41566, South Korea (e-mail: jmkang@knu.ac.kr).

Copyright (c) 20xx IEEE. Personal use of this material is permitted. However, permission to use this material for any other purposes must be obtained from the IEEE by sending a request to pubs-permissions@ieee.org.

II. SYSTEM MODEL

In LoRa, every frame is initiated with a priori known preamble, in which the base chirp \mathbf{x} of size $M \triangleq 2^{\text{SF}}$ is repeated N times, where $\text{SF} \in \mathbb{Z}^+$ is the spreading factor and the base chirp is given by [2], [5]

$$\mathbf{x} = \left\{ e^{j2\pi\left(\frac{m^2}{2M} - \frac{m}{2}\right)} : m = 0, 1, 2, \dots, M-1 \right\} \in \mathbb{C}^M. \quad (1)$$

Suppose that a frame is transmitted over a wireless fading channel denoted by h . Then the problem of LoRa preamble detection can be considered as a binary hypothesis testing problem as follows [2]:

$$\begin{cases} \mathcal{H}_0 : \mathbf{y}_n = \mathbf{w}_n \\ \mathcal{H}_1 : \mathbf{y}_n = \sqrt{\rho}h\mathbf{x} + \mathbf{w}_n \end{cases}, \quad n = 0, 1, \dots, N-1 \quad (2)$$

where $\mathbf{w}_n \in \mathbb{C}^M$ denotes the vector of independent and identically distributed (i.i.d.) Gaussian noises, each with zero mean and variance σ^2 . Also, ρ denotes the transmission power.

III. PROPOSED SCHEME

A. Threshold-Based LoRa Preamble Detection

The basic idea behind the threshold-based preamble detection is that during the consecutive N symbol periods, if the base chirp \mathbf{x} is detected k times, then the presence of the preamble (i.e., \mathcal{H}_1) is declared; otherwise, the absence of preamble (i.e., \mathcal{H}_0) is declared. A useful result for LoRa is that each base chirp in the preamble can be detected based on dechirping, followed by the DFT [3]–[5]. Using this result, in the following, we present a universal algorithm for both coherent and non-coherent procedures of the threshold-based LoRa preamble detection.

Algorithm 1: Threshold-Based LoRa Preamble Detection.

- Step 1) Dechirp the received signals $\{\mathbf{y}_n\}$, followed by taking their DFTs at the 1st frequency bin, as follows:

$$Y_n = \mathbf{1}_M^T (\mathbf{x}^* \odot \mathbf{y}_n), \quad n = 0, 1, \dots, N-1 \quad (3)$$

where $(\cdot)^T$, $(\cdot)^*$, and \odot denote the transpose, complex conjugate, and element-wise product, respectively. Also, $\mathbf{1}_M$ denotes all-one column vector of size M .

- Step 2) Declare the presence of the preamble if

$$\sum_{n=1}^N I(A_n(\gamma)) \geq k \quad (4)$$

where $I(\cdot)$ denotes the indicator function, which is equal to one if the argument is true and is zero otherwise. Also,

$$A_n(\gamma) = \begin{cases} \text{Re}\{h^* Y_n\} \geq \gamma, & \text{coherent detection;} \\ |Y_n| \geq \gamma, & \text{non-coherent detection,} \end{cases} \quad (5)$$

where $\text{Re}\{\cdot\}$ and $|\cdot|$ denote the real part and absolute value of a complex-valued argument, respectively. In addition, γ denotes a threshold for detecting the base chirp \mathbf{x} in each symbol period, and k denotes a threshold for the number of times the base chirp is detected during the N symbol periods.

In the threshold-based preamble detection in Algorithm 1, there are two kinds of detection thresholds, namely, k and γ . In the following, we will optimize the values of k and γ to further improve the performance of the preamble detection.

B. Optimization of Thresholds

To optimize the thresholds, we first have the following results.

Proposition 1: For Algorithm 1, the preamble detection probability (i.e., the probability of correctly detecting the preamble when it is present) is given by

$$P_D(k, \gamma) = \sum_{i=k}^N \binom{N}{i} (p(\gamma))^i (1 - p(\gamma))^{N-i} \quad (6)$$

where

$$p(\gamma) = \begin{cases} Q\left(\sqrt{\frac{2}{|h|^2 \rho \sigma^2}} \gamma - \sqrt{\frac{2|h|^2 \rho}{\sigma^2}}\right), & \text{coherent detection;} \\ Q_1\left(\sqrt{\frac{2|h|^2 \rho}{\sigma^2}}, \sqrt{\frac{2}{|h|^2 \rho \sigma^2}} \gamma\right), & \text{non-coherent detection.} \end{cases} \quad (7)$$

In (7), $Q(\cdot)$ and $Q_1(\cdot, \cdot)$ denote the Q-function and the Marcum Q-function, respectively. Also, the false alarm rate (i.e., the probability of wrongly detecting the preamble when it is absent) is given by

$$P_F(k, \gamma) = \sum_{i=k}^N \binom{N}{i} (q(\gamma))^i (1 - q(\gamma))^{N-i} \quad (8)$$

where

$$q(\gamma) = \begin{cases} Q\left(\sqrt{\frac{2}{|h|^2 \rho \sigma^2}} \gamma\right), & \text{coherent detection;} \\ \exp\left(-\frac{\gamma^2}{|h|^2 \rho \sigma^2}\right), & \text{non-coherent detection.} \end{cases} \quad (9)$$

Proof: First, let us consider the case of coherent detection. Since $Y_n = \mathbf{x}^H \mathbf{y}_n$, it follows from (1)–(3) that $\text{Re}\{h^* Y_n\}$ is a real-valued Gaussian random variable with mean $\mu \triangleq |h|^2 \rho$ and variance $\varsigma^2 \triangleq \frac{|h|^2 \rho \sigma^2}{2}$ under \mathcal{H}_1 , whereas with zero mean and variance ς^2 under \mathcal{H}_0 . Thus, the probabilities of detecting the base chirp \mathbf{x} under \mathcal{H}_1 and \mathcal{H}_0 can be, respectively, derived as $p(\gamma) = Q\left(\sqrt{\frac{2}{|h|^2 \rho \sigma^2}} \gamma - \sqrt{\frac{2|h|^2 \rho}{\sigma^2}}\right)$ and $q(\gamma) = Q\left(\sqrt{\frac{2}{|h|^2 \rho \sigma^2}} \gamma\right)$. Next, we consider the case of non-coherent detection, in which $|Y_n|$ follows a Rayleigh distribution with scale parameter $s \triangleq \sqrt{\frac{|h|^2 \rho \sigma^2}{2}}$ under \mathcal{H}_0 ; whereas, under \mathcal{H}_1 , it follows a Rician distribution with non-centrality parameter $\nu \triangleq |h|^2 \rho$ and spread parameter s . Thus, the values of $p(\gamma)$ and $q(\gamma)$ can be, respectively, obtained as $p(\gamma) = Q_1\left(\sqrt{\frac{2|h|^2 \rho}{\sigma^2}}, \sqrt{\frac{2}{|h|^2 \rho \sigma^2}} \gamma\right)$ and $q(\gamma) = \exp\left(-\frac{\gamma^2}{|h|^2 \rho \sigma^2}\right)$. For both cases of coherent and non-coherent detection, $A_n(\gamma)$'s are i.i.d. Bernoulli random variables with success probability of $p(\gamma)$ under \mathcal{H}_1 ; whereas, with $q(\gamma)$ under \mathcal{H}_0 . Thus, $\sum_{n=1}^N I(A_n(\gamma))$ is a binomial random variable with a probability mass function given by $\Pr(A_n(\gamma) = i | \mathcal{H}_1) = \binom{N}{i} (p(\gamma))^i (1 - p(\gamma))^{N-i}$ under \mathcal{H}_1 or $\Pr(A_n(\gamma) = i | \mathcal{H}_0) = \binom{N}{i} (q(\gamma))^i (1 - q(\gamma))^{N-i}$ under \mathcal{H}_0 . From this, the preamble detection probability and false alarm rate can be obtained as in (6) and (8), respectively. ■

Our goal in this letter is to maximize the preamble detection probability $P_D(k, \gamma)$ under a constraint on the false alarm rate $P_F(k, \gamma)$ by optimizing the detection thresholds k and γ as follows:

$$(P1): \underset{1 \leq k \leq N, \gamma}{\text{maximize}} \quad P_D(k, \gamma) \quad \text{subject to} \quad P_F(k, \gamma) \leq \alpha$$

where α is the maximum tolerance for the false alarm rate. Note that the above problem is non-convex; nonetheless, in the following, we derive its optimal solution by leveraging useful properties of $P_D(k, \gamma)$ and $P_F(k, \gamma)$ derived in Proposition 1.

Proposition 2: The optimal solution to problem (P1) is given by

$$k^* = \underset{1 \leq k \leq N}{\text{argmax}} \quad P_D(k, g(k, \alpha)), \quad (10)$$

$$\gamma^* = g(k^*, \alpha) \quad (11)$$

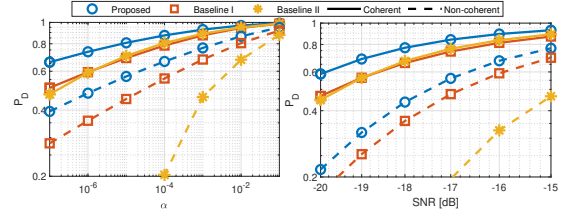


Fig. 1. Preamble detection probability versus α and SNR.

where $g(k, \alpha)$ is the inverse function of $P_F(k, \gamma) = \alpha$ with respect to γ for a given k , i.e., $g(k, \alpha)$ corresponds to the value of γ such that $P_F(k, \gamma) = \alpha$.

Proof: Given k , both $P_D(k, \gamma)$ and $P_F(k, \gamma)$ are monotonically decreasing in γ . Thus, the value of γ maximizing $P_D(k, \gamma)$ while satisfying $P_F(k, \gamma) \leq \alpha$ takes the form of $\gamma = g(k, \alpha)$. Applying this result, (P1) becomes an unconstrained problem to maximize $P_D(k, g(k, \alpha))$ over k . Thus, the optimal value of k can be determined as in (10). Also, by substituting (10) into $g(k, \alpha)$, the result of (11) can be obtained. ■

Notice that it is possible to determine the values of k^* and γ^* efficiently via two- and one-dimensional searching, respectively, of which complexities are given by $\log(N\epsilon^{-1})$ and $\log(\epsilon^{-1})$, where ϵ denotes a computational tolerance for searching γ .

IV. SIMULATION RESULTS

In the simulations, we set SF = 7 and $N = 8$. The signal-to-noise ratio (SNR) is defined as $\frac{M\rho}{\sigma^2}$. Also, the value of h is generated randomly following the circularly symmetric complex Gaussian distribution with zero mean and unit variance. For the purpose of performance comparisons, we evaluate the performance of the following two baseline schemes as extensions of the existing schemes in [3]–[5]:

- **Baseline I:** Algorithm 1 with a fixed value of k arbitrarily chosen between 1 and N (denoted by k'), and with an optimized value of γ maximizing $P_D(k', \gamma)$ under $P_F(k', \gamma) \leq \alpha$. The value of k' is set to vary over every 100 channel realizations.
- **Baseline II:** Algorithm 1 with a fixed value of γ set as intersection between $p(\gamma)$ and $q(\gamma)$ (denoted by γ') and an optimized value of k maximizing $P_D(k, \gamma')$ under $P_F(k, \gamma') \leq \alpha$.

In Fig. 1, the performance of the proposed and baseline schemes (averaged over 10,000 different channel realizations) is compared. In the left sub-figure (resp. right sub-figure) of Fig. 1, the preamble detection probability is plotted versus the value of α when the SNR is -15 dB (resp. versus the SNR when $\alpha = 10^{-3}$). From Fig. 1, it can be seen that the proposed scheme performs much better than the baseline schemes due to the joint optimization of both the two detection thresholds k and γ . The performance gain is observed to be more pronounced in regime of low SNR and/or small α .

V. CONCLUSION

The performance of the threshold-based LoRa preamble detection was significantly improved by optimizing the two detection thresholds, of which superiority was demonstrated by the simulation results.

REFERENCES

- [1] U. Raza *et al.*, “Low power wide area networks: An overview,” *IEEE Commun. Surv. Tuts.*, vol. 19, no. 2, pp. 855–873, 2nd Quart. 2017.
- [2] J.-M. Kang, D.-W. Lim, and K.-M. Kang, “On the LoRa modulation for IoT: Optimal preamble detection and its performance analysis,” *IEEE Internet of Things J.*, vol. 9, no. 7, pp. 4973–4986, Apr. 2022.
- [3] R. Ghanaatian, O. Afisiadis, M. Cotting, and A. Burg, “LoRa digital receiver analysis and implementation,” *arXiv:1811.04146*, 2019.
- [4] J. Tapparel, O. Afisiadis, P. Mayoraz, A. Balatsoukas-Stimming, and A. Burg, “An open-source LoRa physical layer prototype on GNU radio,” *arXiv:2002.08208v2*, 2020.
- [5] M. Xhonneux, O. Afisiadis, D. Bol, and J. Louveaux, “A low-complexity LoRa synchronization algorithm robust to sampling time offsets,” *IEEE Internet of Things J.*, vol. 9, no. 5, pp. 3756–3769, Mar. 2022.